Journal of Chromatography A, 1217 (2010) 1647–1653

Contents lists available at ScienceDirect

Journal of Chromatography A

journal homepage: www.elsevier.com/locate/chroma

Using reversed-phase liquid chromatography to monitor the sizes of Au/Pt core/shell nanoparticles

Fu-Ken Liu[a,*], Yu-Cheng Chang[b]

[a] Department of Applied Chemistry, National University of Kaohsiung, No. 700, Kaohsiung University Road, Nan Tzu District, Kaohsiung 811, Taiwan
[b] Department of Materials Science and Engineering, National Tsing-Hua University, 101, Section 2 Kuang Fu Road, Hsinchu 300, Taiwan

ARTICLE INFO

Article history:
Received 22 October 2009
Received in revised form 5 January 2010
Accepted 11 January 2010
Available online 18 January 2010

Keywords:
Au/Pt
Core/shell
Nanoparticles
Reversed-phase liquid chromatography

ABSTRACT

This paper describes the use of reversed-phase liquid chromatography (RPLC) to rapidly characterize Au/Pt core/shell nanoparticles (NPs) produced through seed-assisted synthesis. We monitored the sizes of Au/Pt core/shell NPs by using a porous silica-based RPLC column (pore size: ca. 100 nm) and 30 mM sodium dodecyl sulfate in deionized water as the mobile phase; the plot of the retention time with respect to the logarithm of the size of the Au NPs was linear (R^2 = 0.997) for diameters falling in the range from 5.3 to 40.1 nm; from five consecutive runs, the relative standard deviations of these retention times were less than 0.4%. We used the optimal separation conditions of the RPLC system to study the effects that the rate of addition of the reducing agent and the volumes of the seed, shell precursor metal ion, and reducing agent solutions had on the sizes of the Au/Pt core/shell NPs. A good correlation existed between the sizes of the Au/Pt core/shell NPs determined through RPLC and those determined using transmission electron microscopy. RPLC appears to be a useful technique for monitoring the sizes of NPs and nanomaterials in general.

1. Introduction

Metal nanoparticles (NPs) are attracting a great deal of attention from practitioners in a wide variety of scientific fields [1–6]. Because the physical and chemical properties of NPs are directly related to their chemical compositions, sizes, and surface structural characteristics [7–10], the design, synthesis, and characterization of nanostructures have become very important aspects of the emerging field of nanomaterials, where macroscopic properties are directly influenced by subtle nanostructural changes. Among the many metals currently under investigation for their nanomaterial properties, platinum (Pt) is one of the mostly researched noble metals because it is widely used in the fabrication of biosensors, in fuel cell technology, and as an effective catalyst for many industrial reactions [11–16].

The particle size effect is related to the variation of a reaction rate, selectivity, and/or sensitivity with respect to the characteristic dimensions of metallic clusters at the electrified solid–liquid interface [17–20]. Therefore, the design and synthesis of Pt nanostructures having well controlled sizes or shapes is of critical importance for their successful application, especially in the field of catalysis [21–24].

In a previous study, we prepared core/shell Au/Pt NPs through "seed-assisted synthesis," a successive reduction process that is effective for the size-controlled synthesis of Pt metal NPs [25]. The seed-assisted synthesis of Au/Pt NPs involves reducing Pt ions on the surfaces of preformed Au seeds – using a mild reducing agent (e.g., ascorbic acid) [25] – by minimizing the degree of nucleation while maximizing particle growth to achieve a shell of uniform thickness. Because the size of the core (seed) is predetermined, the overall dimensions of the core/shell NPs are dependent upon the thickness of the shell material.

When a set number of preformed seeds is used as nucleation centers for the fabrication of core/shell NPs, the NP growth conditions can be controlled simply through varying the fabrication parameters—e.g., the ratio of seeds to the shell metal precursor ions [1] or the rate of addition of the reducing agent [26]. Because there are other important parameters that influence the final sizes and shapes of core/shell NPs, when developing a new medium for the core/shell NP synthesis, it would be ideal if the final NP products could be characterized rapidly in terms of their final sizes to provide feedback so that the synthetic conditions could be optimized.

Reversed-phase liquid chromatography (RPLC) has been employed recently to separate and characterize water-soluble NPs [27]. After using transmission electron microscopy (TEM) to calibrate NP standards, RPLC analysis can then be applied as a stand-alone technique to determine the sizes of synthetic NPs. The prevalence of automated LC systems suggests that, in some instances, such approaches might be superior to other techniques

* Corresponding author. Tel.: +886 7 5919495; fax: +886 7 5919348.
E-mail address: fkliu@nuk.edu.tw (F.-K. Liu).

0021-9673/$ – see front matter © 2010 Elsevier B.V. All rights reserved.
doi:10.1016/j.chroma.2010.01.032

typically employed for the characterization of NPs, such as dynamic light scattering (DLS) [28,29] and TEM [30,31].

Core/shell NPs exhibit a variety of properties depending on the nature of their components and their thicknesses. For example, the high electrocatalytic activities of Pt NPs toward many molecules can be adjusted by changing the thickness of the Pt shell of Au/Pt core/shell NPs [32,33]; therefore, before investigating their applicability, it would be useful to determine the NPs' sizes to establish the relationship between the catalytic behavior and the NP size. Because LC is a rapid, economical technique for separating NPs, we suspected that it might allow us to efficiently determine the size phenomena of fabricated Au/Pt core/shell NPs. Therefore, in this study, we investigated the effects of several important parameters – the rate of addition of the reducing agent and the volumes of the added seeds, shell metal ion precursor, and reducing agent solutions in the reaction medium – on the RPLC separations and sizes of Au/Pt NPs fabricated through seed-assisted synthesis. Because TEM is an accurate reference method for observing the morphologies of NPs [30], we also compared the accuracies of using RPLC- and TEM-based methods to characterize the sizes of Au/Pt core/shell NPs.

2. Experimental

2.1. Apparatus

A Hitachi L-2000 liquid chromatography system (Tokyo, Japan) was used for RPLC separation of the NPs. The RPLC apparatus was equipped with a diode array detection (DAD) system. A Nucleosil C_{18} column (Macherey-Nagel, Duren, Germany; 250 mm × 4.6 mm; pore size: 100 nm; particle size: 7 μm) and a 0.2-μm pre-column filter were employed for analytical separation, using a mobile phase of 30 mM sodium dodecyl sulfate (SDS) in deionized water at a flow rate of 1.0 mL min^{-1}; the detection wavelength was 520 nm and the injection volume was 20 μL. To confirm the accuracy of the size characterization by RPLC, a JEOL JEM-2010 transmission electron microscope (Tokyo, Japan) was used to independently analyze the Au/Pt core/shell NPs. A KDS 100 syringe pump (KD Scientific, Holliston, MA, USA) was used during the synthesis of the NPs.

2.2. Chemical reagents

Hydrogen tetrachloroaurate ($HAuCl_4$) and hydrogen hexachloroplatinate (H_2PtCl_6) were purchased from Acros Organics (Geel, Belgium). Ascorbic acid and sodium citrate were obtained from Merck (Darmstadt, Germany). SDS was obtained from Tokyo Chemical Industry (Tokyo, Japan). Standard Au NPs having a mean diameter of 5.3 nm [standard deviation (SD): 0.5 nm] were obtained from Sigma (St. Louis, MO, USA). Au NPs having mean diameters of 40.1 nm (SD: 3.2 nm) were obtained from BB International (Cardiff, UK). All eluents were prepared afresh each day and filtered through a 0.45-μm nylon membrane filter (Alltech, Deerfield, IL, USA) prior to use. Deionized water (>18 MΩ cm^{-1}) was used throughout the experiments.

2.3. Preparation of Au NPs

The synthetic procedure for the formation of smaller-sized Au NPs through citrate-mediated reduction of $HAuCl_4$ has been described elsewhere [28]. The resulting Au NPs were spherical; after digitizing TEM images, 2D-grain analysis revealed particle diameters of 12.1 ± 0.9 nm.

For the preparation of larger-sized Au NPs, two 20-mL sample vials (labeled A and B, respectively) were charged with deionized water (10 mL); a volume of 12.1-nm Au NPs (serving as seeds: 0.3 mL in A; 0.1 mL in B) was added to each vial, followed by $HAuCl_4$ solution (3.0×10^{-3} M, 0.5 mL). While the solutions were stirring, ascorbic acid (1.0×10^{-2} M, 0.5 mL) was added slowly (0.5 mL min^{-1}) from a burette to each vial. The resulting solutions were then stirred for 30 min. These procedures were performed at room temperature (ca. 25 °C). The resulting Au NPs were spherical; after digitizing TEM images, 2D-grain analysis revealed particle diameters for samples A and B of 21.2 ± 3.6 and 29.4 ± 3.1 nm, respectively.

2.4. Seed-assisted synthesis of Au/Pt core/shell NPs: varying the rate of addition of the reducing agent

Three 20-mL sample vials (labeled C–E, respectively) were charged sequentially with deionized water (7.5 mL), 12.1-nm Au seeds (0.75 mL), and H_2PtCl_6 solution (1.0×10^{-3} M, 2.5 mL). Ascorbic acid (1.0×10^{-2} M, 0.5 mL) was added to each vial via a syringe pump (operated at rates of 5.0, 200, and 2000 mL h^{-1} for vials C–E, respectively), while stirring. Finally, SDS (8.0×10^{-2} M, 10 mL) was added to each vial and the resulting solutions stirred for 30 min. These procedures were performed at room temperature (ca. 25 °C).

2.5. Seed-assisted synthesis of Au/Pt core/shell NPs: in the presence of various seed volumes

Two 20-mL sample vials (labeled F and G, respectively) were charged sequentially with deionized water (7.5 mL), 12.1-nm Au seeds (1.0 and 0.4 mL for vials F and G, respectively), and H_2PtCl_6 solution (1.0×10^{-3} M, 2.5 mL). Ascorbic acid (1.0×10^{-2} M, 0.5 mL) was added to each vial via syringe pump (at a rate of 5.0 mL h^{-1}), while stirring. Finally, SDS (8.0×10^{-2} M, 10 mL) was added to each vial and the resulting solutions stirred for 30 min. These procedures were performed at room temperature (ca. 25 °C).

2.6. Seed-assisted synthesis of Au/Pt core/shell NPs: in the presence of various volumes of shell precursor metal ions

Two 20-mL sample vials (labeled H and I, respectively) were charged sequentially with deionized water (7.5 mL), 12.1-nm Au seeds (1.0 mL), and H_2PtCl_6 solution (1.0×10^{-3} M; 4.5 and 5.5 mL for vials H and I, respectively). Ascorbic acid (1.0×10^{-2} M, 0.5 mL) was added to each vial via a syringe pump (at a rate of 5.0 mL h^{-1}), while stirring. Finally, SDS (8.0×10^{-2} M, 10 mL) was added to each vial and the resulting solutions stirred for 30 min. These procedures were performed at room temperature (ca. 25 °C).

2.7. Seed-assisted synthesis of Au/Pt core/shell NPs: in the presence of various volumes of reducing agent

Three 20-mL sample vials (labeled J–L, respectively) were charged sequentially with deionized water (7.5 mL), 12.1-nm Au seeds (1.0 mL), and H_2PtCl_6 solution (1.0×10^{-3} M, 2.5 mL). Ascorbic acid (1.0×10^{-2} M; 0.5, 1.0, and 1.5 mL for J–L, respectively) was added to each vial via a syringe pump (at a rate of 5.0 mL h^{-1}), while stirring. Finally, SDS (8.0×10^{-2} M, 10 mL) was added to each vial and the resulting solutions stirred for 30 min. These procedures were performed at room temperature (ca. 25 °C).

3. Results and discussion

3.1. Evaluation of the formation of Au/Pt NPs by seed-assisted synthesis

Before employing RPLC to study the sizes and size distributions of the Au/Pt core/shell NPs, we first confirmed that it was possible

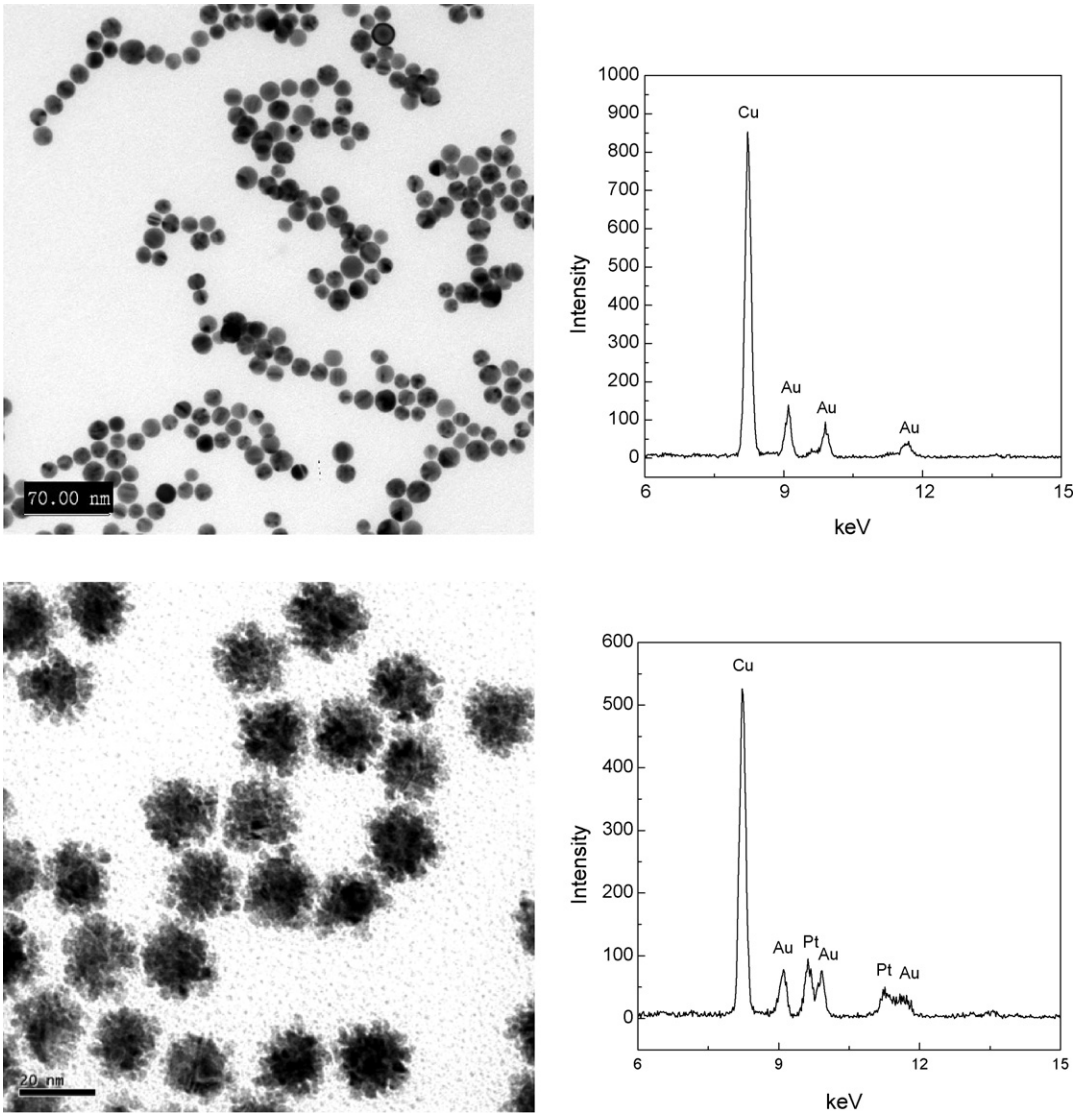

Fig. 1. (a) Left: TEM image of Au seeds; right: EDS spectrum of the sample. (b) Left: TEM image of Au/Pt NPs; right: EDS spectrum of the sample.

to produce Au/Pt core/shell NPs using the seed-assisted synthesis strategy. In the core/shell NP fabrication process, the colors of the solutions changed gradually from red (prior to synthesis) to brown-gray (after the synthesis). This color transformation is indicative of the chemical reduction of H_2PtCl_6 and the deposition of Pt onto the surfaces of the Au seeds [32]. A TEM image (Fig. 1a, left) recorded prior to performing the synthesis reveals that the Au seeds were spherical and had a quite-uniform size distribution. The average particle size of the seeds, determined through 2D-grain analysis after digitizing the TEM images, was 12.1 ± 0.9 nm. We used energy dispersive spectroscopy (EDS; Fig. 1a, right) to confirm that the seeds were composed of Au; the signal for Cu in the EDS spectrum was due to the use of a Cu grid as the sample holder in TEM analysis. After completing the fabrication procedure for sample C (see Section 2 for the fabrication procedure), the TEM image (Fig. 1b, left) revealed that its size distribution was also uniform. These particles appeared to have a "custard apple" morphology, similar to that of the Au/Pt NPs fabricated by Fan et al. [34]. The average particle size, determined through 2D-grain analysis after digitizing the TEM image, was 18.3 ± 2.4 nm. The EDS analysis (Fig. 1b, right) reveals that the particles in sample C comprised Au and Pt elements (again, the signal for Cu arose from the use of a Cu grid as a sample holder). Thus, seed-assisted synthesis appears to be a useful method for the fabrication of Au/Pt core/shell NPs.

3.2. Separation of NP standards using RPLC

In this study, we used standard sized Au NPs to calibrate the column used to separate the Au/Pt core/shell NPs. We selected Au NPs standards because they are commercially available and possess very narrow size distributions (several nanometers).

Surfactants can be employed as stabilizers for the size-selective preparation of metal particles [35,36]. Kondow et al. [37] and Chen and Yeh [38] demonstrated that SDS has a positive stabilizing effect on NPs. Such ionic surfactants surround the metal NPs (or core/shell bimetallic NPs), preventing their agglomeration through electrostatic repulsion [39]. Therefore, we used SDS as a mobile phase additive to improve the stability of our NPs during the separation process.

The use of SDS as a mobile phase additive in the size-related separation of NPs has another interesting function. Bettmer et al. reported that the separation of Au NPs through RPLC required the addition of SDS as a mobile phase additive (ca. 10 mM in their case)

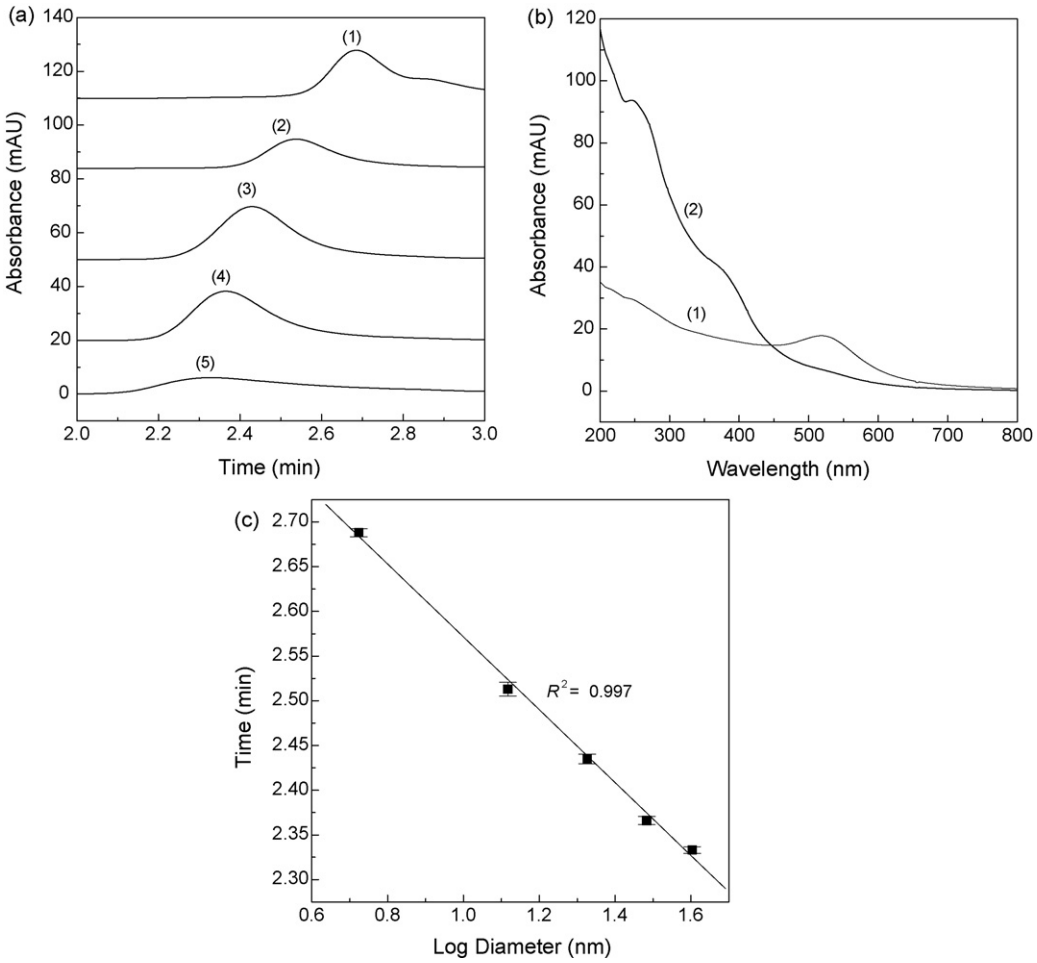

Fig. 2. (a) Chromatograms of five differently sized Au NPs, eluted with 30 mM SDS in deionized water. Other conditions are described in Section 2. Peaks: (1) = 5.3 nm; (2) = 12.1 nm; (3) = 21.2 nm; (4) = 29.4 nm; (5) = 40.1 nm. (b) UV–vis absorption spectra of the signals in (a) set (1), obtained at elution times of (1) 2.68 and (2) 2.87 min. (c) Calibration curve for the elution time of Au NPs plotted with respect to the logarithm of their diameter. Error bars in the *y* dimension represent the variations of the elution times in terms of one standard deviation.

to prevent irreversible adsorption of the NPs on the packing material [27]. Herein, we selected an SDS concentration of 30 mM as the mobile phase additive for our investigation of the use of RPLC for NP separations.

First, we evaluated the feasibility of performing the size-based separation of NPs through RPLC. We separated Au NPs of five different sizes (5.3, 12.1, 21.2, 29.4, and 40.1 nm) using a mobile phase of 30 mM SDS in deionized water at a flow rate of 1.0 mL min^{-1}. The chromatograms in Fig. 2a indicate that the five differently sized Au NPs had different elution times, ranging from 2.33 to 2.68 min; the increasing elution times upon decreasing the Au NP size parallels elution behavior described previously [27]. The peak widths in Fig. 2a (ca. 0.3 min) are similar to those (ca. 0.35 min) reported by Bettmer et al. [27]. In a previous study, we demonstrated that the peak widths of NPs in liquid chromatograms are strongly related to their size distributions [26]; namely, a larger size distribution of NPs will result in a wider peak in a chromatogram. Therefore, the peak shapes are not solely affected by the elution times—they are also affected by the size distribution.

Notably, the chromatogram of set (1) in Fig. 2a reveals two peaks. The 5.3-nm Au NPs standard that we had purchased had been produced through the reduction of a Au metal ion precursor solution with a mixture of trisodium citrate and tannic acid [40]. In the separation of NPs, UV–vis absorption spectra obtained from a DAD can provide information relating to the elution of the NPs [41]. In this study, we used a DAD to record all wavelengths simultaneously during the elution process. Fig. 2b presents the corresponding UV–vis absorption spectra obtained when sampling the chromatogram at different elution times. At an elution time of 2.68 min, Fig. 2b set (1) reveals a surface plasmon resonance (SPR) peak at 517 nm, which is indicative of 5.3-nm Au NPs [42]. At an elution time of ca. 2.87 min, Fig. 2b set (2) reveals no such SPR peak of Au NPs; i.e., no 5.3-nm Au NPs were present in the sample matrix (a mixture of trisodium citrate and tannic acid) passing through the detection window of the DAD. By monitoring the spectra obtained at the individual elution times, we assign the species that migrated more quickly (ca. 2.68 min) to the 5.3-nm Au NPs; the more slowly eluting species (ca. 2.87 min) was merely the sample matrix of the Au NPs.

For RPLC to be used practically for the routine analysis of NP sizes, it was necessary for us to validate the reproducibility of the elution times—because it influences the precision of the size characterization process. Thus, we measured the relative standard deviations of the elution times from five consecutive runs using the 5.3-, 12.1-, 21.2-, 29.4-, and 40.1-nm-diameter Au NP standards; the calculated precisions were 0.17, 0.31, 0.22, 0.19, and 0.16%, respectively. These results indicate that RPLC provides good reproducibility of the elution behavior of Au NPs.

Fig. 2c indicates that a strong correlation (R^2 = 0.997) exists between the elution time and the logarithm of the size of the NPs; the error bars for the *y*-axis reveal the variations in elution times at one standard deviation. This plot confirms that it is possible to

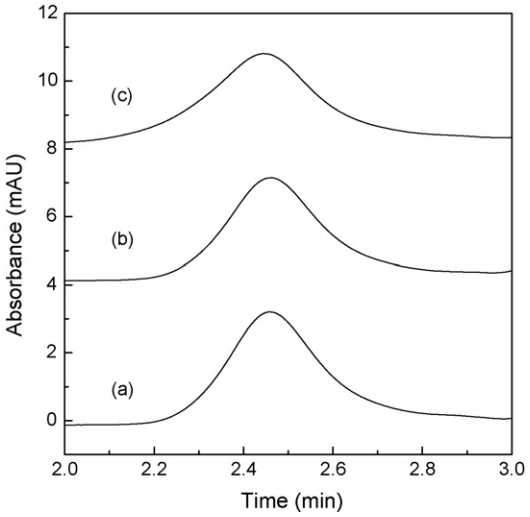

Fig. 3. RPLC chromatograms of Au/Pt core/shell NPs solutions synthesized using different rates of addition of the reducing agent. Synthetic conditions for preparing these Au/Pt NPs and their separation conditions are described in Section 2. (a) Sample C; (b) sample D; (c) sample E.

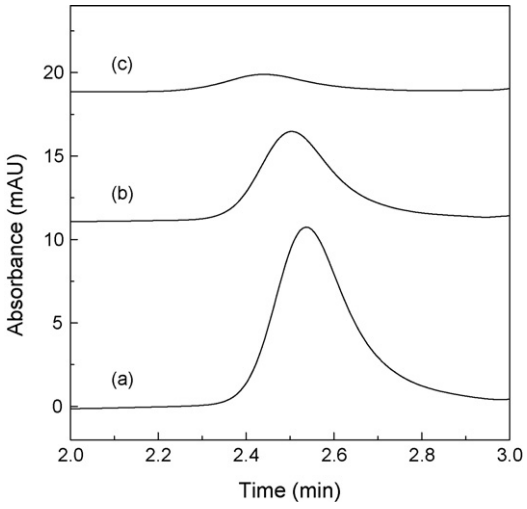

Fig. 4. RPLC chromatograms of the Au/Pt core/shell NPs solutions synthesized using various concentrations of seed Au NPs. Synthetic conditions for preparing these Au/Pt NPs and their separation conditions are described in Section 2. (a) 12.1-nm Au seeds; (b) Sample F; (c) Sample G.

employ RPLC to characterize NPs having sizes in the nanometer regime.

3.3. Effect of rate of ascorbic acid addition on the fabrication of Au/Pt NPs

In a previous study, we examined the feasibility of fabricating Au NPs using the seed-assisted synthesis strategy; we found that employing the same quantities of the reducing agent, seeds, and precursor metal ions, but varying the rate of addition of the reducing agent, significantly affected the sizes of the final Au NPs [26]. Indeed, the key feature affecting the fabrication of Au NPs with controllable size distributions was the rate of addition of the reducing agent. Therefore, in this present study, we investigated whether the rate of addition of ascorbic acid also influenced the final sizes and size distributions of the Au/Pt core/shell NPs.

During chromatographic separations, the solute in the column spreads into a Gaussian shape; the peak width at half maximum ($w_{1/2}$) of the Gaussian peak is equal to 2.35 times the standard deviation [43]. Thus, if we know the elution time and the value of $w_{1/2}$ from the RPLC chromatogram of the NPs, the size calibration curve of the standard NPs will provide the mean sizes and size distributions of the fabricated core/shell NPs. The RPLC chromatograms in Fig. 3 suggest that the eluted samples C–E contained Au/Pt core/shell NPs having mean diameters (plus one standard deviation) of ca. 18.9 ± 4.4, 18.9 ± 4.5, and 20.4 ± 9.6 nm, respectively. Thus, RPLC analysis revealed that the mean size of the Au/Pt core/shell NPs increased slightly upon increasing the rate of addition of the reducing agent. We note, however, that the Au/Pt core/shell NPs in sample E were relatively polydisperse when compared with samples C and D, suggesting that they had formed through heterogeneous growth [1]; i.e., the formation of new nucleation centers presumably occurred simultaneously with seed-assisted synthesis of the Au/Pt core/shell NPs in sample E. Therefore, rapid addition of the reducing agent did not produce Au/Pt core/shell NPs having a narrow size distribution.

Taken together, the RPLC analyses in Fig. 3 reveal that seed-assisted synthesis provided Au/Pt core/shell NPs having a narrower size distribution when the rate of addition of the reducing agent into the synthesis vial was slower.

3.4. Effect of seed volume on the fabrication of Au/Pt NPs

Ideally, for successful seed-assisted synthesis of NPs, the seeds must act as nucleation centers that grow through reduction of the precursor metal ions on the NP surfaces. With fewer seed NPs present, the number of precursor metal ions adsorbed per seed particle increases. Therefore, after reduction of the adsorbed precursor metal ions, the shell thickness increases and, hence, the particle size increases [44]. Thus, we investigated whether the addition of different seed volumes would affect the growth of the Au/Pt core/shell NPs.

Fig. 4 presents RPLC chromatograms of the Au/Pt core/shell NPs in samples F and G. The elution times for the Au/Pt core/shell NPs in these samples were shorter than that of the 12.1-nm Au seeds (Fig. 4a); the elution time of the NPs in sample F (Fig. 4b) was longer than that for sample G (Fig. 4c). These chromatograms reveal several phenomena. First, the fabricated Au/Pt core/shell NPs were larger than the Au seeds, consistent with the Pt shell precursor metal ions having been deposited onto the surfaces of the Au seed particles; i.e., growth of the Au/Pt core/shell NPs occurred through seed-assisted synthesis. Second, a smaller Au seed volume produced larger Au/Pt core/shell NPs, consistent with a larger number of precursor metal ions having been adsorbed onto and reduced on each Au seed particle [44].

According to the size calibration curve for the RPLC separations, the elution times and peak widths suggested that the Au/Pt core/shell NPs in samples F and G had mean diameters (plus one standard deviation) of ca. 14.6 ± 1.6 and 21.3 ± 4.2 nm, respectively. Therefore, we conclude that the mean diameter of the Au/Pt core/shell NPs increased upon decreasing the number of seeds. This finding is consistent with previous results [44]; it demonstrates that, when using seed-assisted synthesis for the fabrication of Au/Pt core/shell NPs, the final sizes of the NPs can be controlled by adding a suitable number of seed NPs to the reaction vial [28].

3.5. Effect of the volume of precursor metal ions on the fabrication of Au/Pt NPs

Ideally, during the seed-assisted synthesis of NPs, a larger ratio of the precursor metal ion volume to the number of seeds would lead to a larger number of metal ions being adsorbed onto each seed particle. Reduction of these adsorbed precursor metal ions

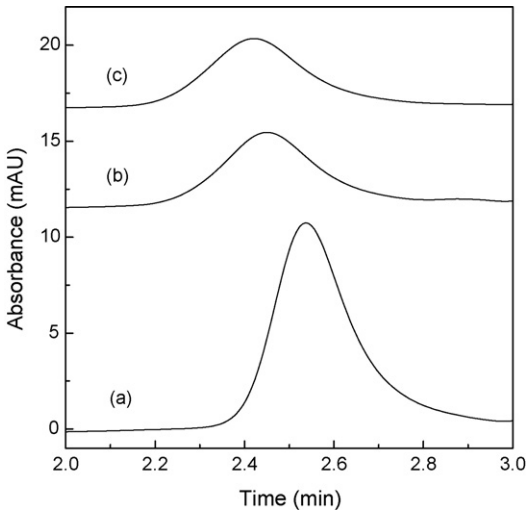

Fig. 5. RPLC chromatograms obtained from Au/Pt NP solutions synthesized through the addition of different volumes of H_2PtCl_6 solution. Synthetic conditions for preparing these Au/Pt core/shell NPs and their separation conditions are described in Section 2. (a) 12.1-nm Au seeds; (b) sample H; (c) sample I.

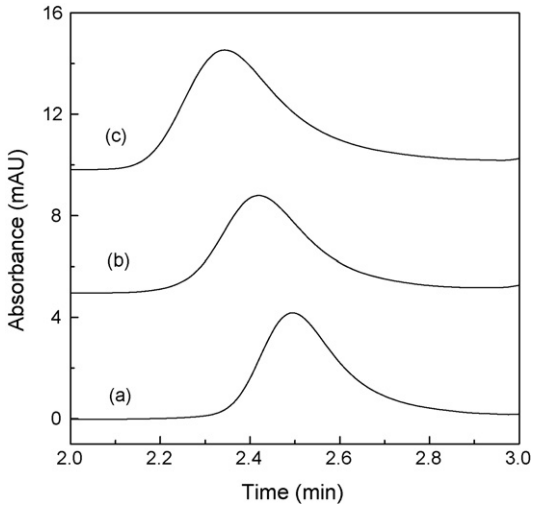

Fig. 6. RPLC chromatograms obtained from Au/Pt core/shell NP solutions synthesized through the addition of different volumes of ascorbic acid solution. Synthetic conditions for preparing these Au NPs and their separation conditions are described in Section 2. (a) Sample J; (b) sample K; (c) sample L.

would increase the shell thickness to produce larger particles [28].

Herein, we investigated whether the addition of different volumes of the precursor metal ion would affect the sizes of the Au/Pt core/shell NPs; we maintained the volume of the solution containing the Au seeds at 1.0 mL and varied the volume of the H_2PtCl_6 solution added to the synthesis medium. Fig. 5 presents RPLC chromatograms of the Au/Pt core/shell NPs in samples H and I. The elution times for the Au/Pt core/shell NPs in these samples were shorter than that of the Au 12.1 nm seeds (Fig. 5a); the elution time of the NPs in sample H (Fig. 5b) was longer than that for sample I (Fig. 5c). Thus, the elution time decreased upon increasing the ratio between the volume of the precursor metal ion solution and the number of seeds. The RPLC chromatograms in Fig. 5 indicate that the NPs that eluted during the analyses of samples H and I had diameters (plus one standard deviation) of ca. 20.1 ± 4.4 and 23.8 ± 5.9 nm, respectively.

From these observations, we conclude that when we increased the volume of Pt metal ions, the additional Pt metal ions were also adsorbed onto the Au seeds and subsequently reduced to Pt(0) by the reducing agent (ascorbic acid), thereby enlarging the final diameters of the NPs through seed-assisted synthesis [28]. Thus, Au/Pt NPs of various sizes can be fabricated simply by modifying the volume of the added Pt metal ions.

3.6. Effect of the volume of ascorbic acid on the fabrication of Au/Pt NPs

In this section, we used RPLC to determine the sizes of the Au/Pt core/shell NPs obtained after the addition of three different volumes of the ascorbic acid solution. As indicated in Fig. 6, the resulting Au/Pt core/shell NP samples had different elution times, which decreased upon increasing the amount of ascorbic acid. Thus, the addition of a suitable amount of ascorbic acid to the synthesis medium can be used to control the sizes of the resulting Au/Pt core/shell NPs. The RPLC chromatograms in Fig. 6 indicate that the NPs that eluted during the analyses of samples J–L had diameters (plus one standard deviation) of ca 15.4 ± 2.2, 23.6 ± 4.9, and 37.0 ± 9.9 nm, respectively. From these observations, we conclude that increasing the volume of ascorbic acid increased the probability of the Pt metal ions adsorbed on the Au seeds being reduced to Pt(0) by ascorbic acid, thereby enlarging the NPs. We also confirmed that the sizes of the NPs could be controlled simply by modifying the volume of ascorbic acid added.

3.7. Comparing RPLC- and TEM-based methods of size characterization

To use the standard Au NP samples as calibration standards for the size separation of Au/Pt core/shell NPs, it was essential for us to test the accuracy of RPLC in determining the sizes of Au/Pt core/shell NPs. Thus, we used TEM to independently analyze sample K, prepared as described in Section 2. After recording the RPLC chromatogram of these Au/Pt core/shell NPs and measuring the elution time and value of $w_{1/2}$ of the signal (Fig. 6b), we used the size calibration curve to determine a mean size and standard deviation of ca. 23.6 ± 4.9 nm.

TEM is a well-established reference method for observing the sizes of NPs [30]. Fig. 7a displays a TEM image of the Au/Pt core/shell NPs used to obtain Fig. 6b. Fig. 7b presents the size histogram of the particles in the sample, determined through 2D-grain analysis after digitizing the TEM image in Fig. 7a; the mean particle diameter in sample K was 24.7 ± 2.5 nm. Comparing the particle sizes determined through TEM and RPLC analyses, via a *t*-test with 95% confidence level, suggested that there was no significant difference between the two methods. Thus, our particle size analysis using TEM (Fig. 7b) was consistent with our findings obtained using RPLC (Fig. 6b). Therefore, we could use the standard Au NP samples to calibrate the column used for the separation of the Au/Pt core/shell NPs.

Using RPLC, the process of characterizing the analytes took less than 4 min (Fig. 6b)—in contrast to the hour or more often required for TEM analysis. By applying this RPLC method for the characterization of Au/Pt core/shell NPs, the overall analysis time was reduced significantly because it omitted the most time consuming process—TEM sample preparation. An additional general advantage that RPLC has over TEM is the lower cost of operation. For these reasons alone, the performance of this RPLC method is superior to existing TEM methods. Taken together, it appears that RPLC-based methods are superior – in terms of accuracy and time – to TEM-based methods for the determination of the sizes of Au/Pt core/shell NPs.

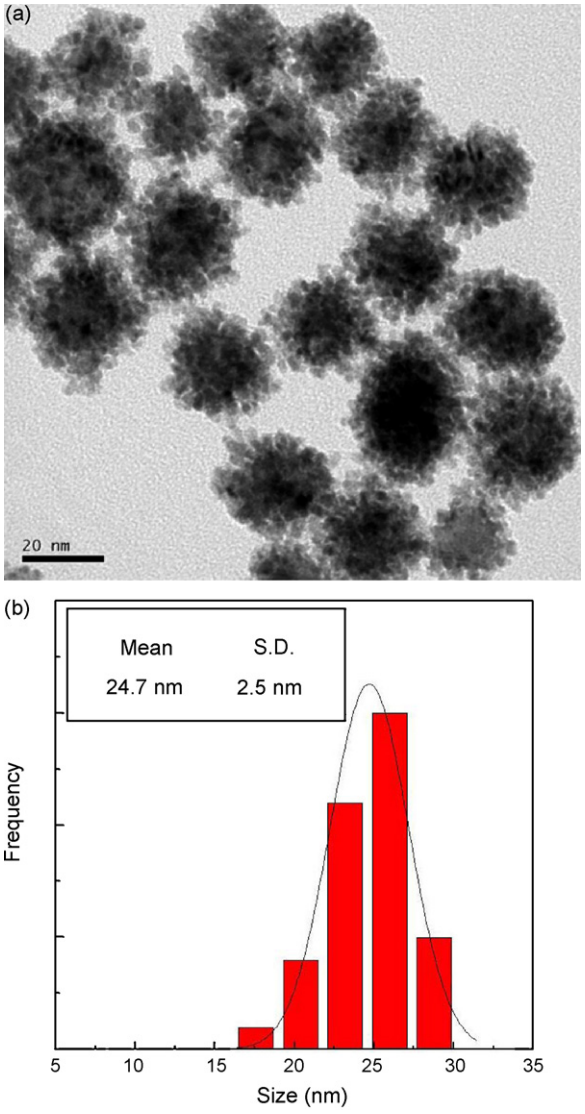

Fig. 7. TEM analysis of the Au/Pt core/shell NPs in sample K: (a) TEM image; (b) size histogram. Synthetic conditions for preparing these Au/Pt core/shell NPs are described in Section 2.

4. Conclusion

RPLC is an effective and rapid method for characterizing the behavior of Au/Pt core/shell NPs, thereby, providing feedback allowing optimization of the synthetic conditions. RPLC-based analyses of NPs are rapid (<4 min) and economical. The accuracy of our developed RPLC method for the size characterization of Au/Pt core/shell NPs is equal to that of TEM-based analysis; the excellent correlation between these two methods suggests that RPLC is a preferable and more-attractive tool for the routine analyses of the sizes of nanocomposites. Our results demonstrate that RPLC can be used to rapidly screen the growth of Au/Pt core/shell NPs having diameters in the nanometer-scale regime. We believe that strategies employing RPLC for the analysis of nanocomposites will accelerate the characterization of nanomaterials in the future.

Acknowledgment

This study was supported financially by the National Science Council, Taiwan (NSC 97-2113-M-390-004-MY3).

References

[1] N.R. Jana, L. Gearheart, C.J. Murphy, Chem. Mater. 13 (2001) 2313.
[2] G. Schmid, M. Baumle, M. Geerkens, I. Helm, C. Osemann, T. Sawitowski, Chem. Soc. Rev. 28 (1999) 179.
[3] C.N.R. Rao, G.U. Kulkarni, P.J. Thomas, P.P. Edwards, Chem. Soc. Rev. 29 (2000) 27.
[4] A.C. Templeton, M.P. Wuelfing, R.W. Murray, Acc. Chem. Res. 33 (2000) 27.
[5] S.W. Chen, R.S. Ingram, M.J. Hostetler, J.J. Pietron, R.W. Murray, T.G. Schaaff, J.T. Khoury, M.M. Alvarez, R.L. Whetten, Science 280 (1998) 2098.
[6] C.J. Murphy, Science 298 (2002) 2139.
[7] T.H. Chang, F.K. Liu, Y.C. Chang, T.C. Chu, Chromatographia 67 (2008) 723.
[8] C.A. Mirkin, R.L. Letsinger, R.C. Mucic, J.J. Storhoff, Nature 382 (1996) 607.
[9] A. Taleb, C. Petit, M.P. Pileni, Chem. Mater. 9 (1997) 950.
[10] J.A. Ascencio, H.B. Liu, U. Pal, A. Medina, Z.L. Wang, Microsc. Res. Tech. 69 (2006) 522.
[11] M. Hou, S.J. Sun, Z.L. Jiang, Talanta 72 (2007) 463.
[12] S.B. Zhang, Z.S. Wu, M.M. Guo, G.L. Sheng, R.Q. Yu, Talanta 71 (2007) 1530.
[13] M.A.A. Lomillo, J.G. Ruiz, F.J.M. Pascual, Anal. Chim. Acta 547 (2005) 209.
[14] H.H. Zhou, H. Chen, S.L. Luo, J.H. Chen, W.Z. Wei, Y.F. Kuang, Biosens. Bioelectron. 20 (2005) 1305.
[15] M.H. Yang, F.L. Qu, Y.S. Lu, G.L. Shen, R.Q. Yu, Talanta 74 (2008) 831.
[16] M. Subhramannia, V.K. Pillai, J. Mater. Chem. 18 (2008) 5858.
[17] K.J.J. Mayrhofer, M. Arenz, B.B. Blizanac, V. Stamenkovic, P.N. Ross, N.M. Markovic, Electrochim. Acta 50 (2005) 5144.
[18] K.A. Friedrich, F. Henglein, U. Stimming, W. Unkauf, Colloids Surf. A 134 (1998) 193.
[19] O.V. Cherstiouk, P.A. Simonov, E.R. Savinova, Electrochim. Acta 48 (2003) 3851.
[20] F. Maillard, M. Eikerling, O.V. Cherstiouk, S. Schreier, E. Savinova, U. Stimming, Faraday Discuss. 125 (2004) 357.
[21] R. Narayanan, M.A. El-Sayed, Nano Lett. 4 (2004) 1343.
[22] L.M. Falicov, G.A. Somorjai, Proc. Natl. Acad. Sci. U.S.A. 82 (1985) 2207.
[23] D.R. Rolison, Science 299 (2003) 1698.
[24] M.S. Chen, D.W. Goodman, Catal. Today 111 (2006) 22.
[25] L.H. Lu, G.Y. Sun, H.J. Zhang, H.S. Wang, S.Q. Xi, J.Q. Hu, Z.Q. Tian, R. Chen, J. Mater. Chem. 14 (2004) 1005.
[26] F.K. Liu, Chromatographia 68 (2008) 81.
[27] A. Helfrich, W. Bruchert, J. Bettmer, J. Anal. Atom. Spectrom. 21 (2006) 431.
[28] F.K. Liu, Chromatographia 66 (2007) 791.
[29] A.V. Gaikwad, P. Verschuren, E. Eiser, G. Rothenberg, J. Phys. Chem. B 110 (2006) 17437.
[30] J.P. Wilcoxon, J.E. Martin, P. Provencio, Langmuir 16 (2000) 9912.
[31] F.K. Liu, G.T. Wei, Chromatographia 59 (2004) 115.
[32] L. Qian, Y.F. Sha, X.R. Yang, Thin Solid Films 515 (2006) 1349.
[33] Y.D. Jin, S.J. Dong, J. Phys. Chem. B 107 (2003) 12902.
[34] F.R. Fan, D.Y. Liu, Y.F. Wu, S. Duan, Z.X. Xie, Z.Y. Jiang, Z.Q. Tian, J. Am. Chem. Soc. 130 (2008) 6949.
[35] N. Toshima, T. Takahashis, Bull. Chem. Soc. Jpn. 65 (1992) 400.
[36] Y.Y. Yu, S.S. Chang, C.L. Lee, C.R.C. Wang, J. Phys. Chem. B 101 (1997) 6661.
[37] F. Mafune, J. Kohno, Y. Takeda, T. Kondow, H. Sawabe, J. Phys. Chem. B 104 (2000) 9111.
[38] Y.H. Chen, C.S. Yeh, Colloids Surf. A 197 (2002) 133.
[39] F.K. Liu, Chromatographia 70 (2009) 7.
[40] J.W. Slot, H.J. Geuze, Eur. J. Cell Biol. 38 (1985) 87.
[41] F.K. Liu, F.H. Ko, P.W. Huang, C.H. Wu, T.C. Chu, J. Chromatogr. A 1062 (2005) 139.
[42] S. Link, M.A. El-Sayed, J. Phys. Chem. B 103 (1999) 4212.
[43] D.C. Harris, Quantitative Chemical Analysis, 7th ed., W.H. Freeman, New York, 2007.
[44] M. Mandal, N.R. Jana, S. Kundu, S.K. Ghosh, M. Panigrahi, T. Pal, J. Nanopart. Res. 6 (2004) 53.